2412

Targeting Migration inducing gene-7 inhibits carcinoma cell invasion, early primary tumor growth, and stimulates monocyte oncolytic activity

Aaron P. Petty,[4] Stephen E. Wright,[1,2,3]
Kathleen A. Rewers-Felkins,[1,2]
Michelle A. Yenderrozos,[5] Beth A. Vorderstrasse,[5]
and J. Suzanne Lindsey[4]

[1]Department of Veterans Affairs Medical Center; Women's Health Research Institute, Departments of Internal Medicine, Microbiology and Immunology, and Cell Biology and Biochemistry, Texas Tech University Health Sciences Center, School of Medicine; [2]Harrington Cancer Center; and [3]Department of Pharmaceutical Sciences, Texas Tech University Health Sciences Center School of Pharmacy, Amarillo, Texas; and [4]School of Molecular Biosciences and [5]Department of Pharmaceutical Sciences, College of Pharmacy, Washington State University, Pullman, Washington

Abstract

Expression of Migration inducing gene-7 (Mig-7) is limited to tumor cells and to date not found in normal tissues. Multiple tumor microenvironment factors, such as epidermal and hepatocyte growth factors, in concert with $\alpha v \beta 5$ integrin ligation, induce Mig-7 mRNA expression. Gain or loss of Mig-7 protein studies shows that Mig-7 promotes invasion of colon and endometrial carcinoma cells. These data led us to hypothesize that targeting Mig-7 through various methods could decrease invasion, enhance monocyte cell killing of tumor cells, and inhibit disease progression. To begin testing this hypothesis, an *in vitro* chemoinvasion assay of endometrial carcinoma cells treated with Mig-7–specific or control antibodies was used. Mig-7 antibody significantly reduced invasion by >60% compared with controls. In another approach to test this hypothesis, an *in vitro* analysis of peptide-stimulated human peripheral blood monocyte cells and their killing of MCF-7 breast carcinoma cells was used. Mig-7 peptide treatment increased monocyte cell tumor necrosis factor expression and killing of MCF-7 cells 30-fold over no peptide stimulation and 3-fold over

Requests for reprints: J. Suzanne Lindsey, Washington State University, School of Molecular Biosciences, Pullman, WA 99164. Phone: 206-619-9077; Fax: 206-957-7399. E-mail: lindseys@wsu.edu

MUC-1 or control peptide treatments. Furthermore, stably expressing Mig-7–specific short hairpin RNA resulted in significantly reduced Mig-7 protein levels and early primary tumor growth in a xenograft nude mouse model. Reduced phosphorylation of ERK1/2, Akt, and S6 kinase as well as decreased membrane-type 1 matrix metalloproteinase activity were mechanisms through which Mig-7 protein caused these effects. Based on these collective data, Mig-7 expression could be a potential candidate for future targeted cancer therapies. [Mol Cancer Ther 2009; 8(8):2412–23]

Introduction

Discovery and targeting of tumor cell–specific gene expressions could lead to more effective cancer treatments with less toxic side effects. Furthermore, targeting tumor cell proteins that facilitate their invasion, during which tumor cells are resistant to current therapies (1), could provide additional efficacy and less recurrence of disease. We have discovered one such human protein, Migration inducing gene-7 (Mig-7), which is regulated by tumor microenvironment factors (2–5).

Mig-7 protein is cysteine rich and is primarily localized to the membrane fraction of carcinoma cells. Mig-7 expression, a result of receptor tyrosine kinase (RTK) activation, also requires $\alpha v \beta 5$ integrin ligation (1, 2) that acts in concert with RTK activation causing tumor cell invasion and dissemination *in vivo* (6, 7). Antisense to Mig-7, but not sense, oligonucleotide treatment inhibits carcinoma cell scattering (2). In previous studies to date, 87% of tumors from breast, endometrial, colon, lung, ovary, stomach, kidney, thyroid, cervix, small intestine and prostate ($n > 200$ patients), blood from untreated cancer patients, and metastatic sites possess cells expressing Mig-7 mRNA. Notable from these studies is that Mig-7 mRNA is not detectable in 25 different normal tissues ($n = 6$ each tissue) or in blood from normal subjects (2, 4).

Consistent with Mig-7 expression causing invasion, its cDNA is 99% homologous to expressed sequence tags isolated from early invasive stage placenta (2). During placental development, trophoblast cells from the implanted blastocyst invade through the endometrium and one third of the myometrium. These plastic cells can also mimic endothelial cells to remodel the maternal spiral arteries; a process that provides sufficient blood flow for fetal growth and development. Thus, the only normal cells found to date that express Mig-7 are trophoblast cells (3) that behave like aggressive tumor cells (8–10).

HT29 colon carcinoma cell Mig-7 expression induces invasion and vessel-like structure formation in three-dimensional cultures (3). In addition, Mig-7 expression

in these cells reduces their adhesion to laminin and increases production of laminin 5 γ2 chain promigratory fragments (3) known to promote invasion and vessel-like structure formation by aggressive melanoma cells (11). Furthermore, knockdown of Mig-7 by stable shRNA expression in RL95 endometrial carcinoma cells causes reduced invasion in three-dimensional cultures (3).

In vivo, tumor cells can line lumens of irregular vessels in multiple tumor types, including melanoma, ovarian carcinoma, Ewing sarcoma, and hepatocarcinoma (12–15). In three-dimensional cultures, aggressive melanoma cells have been found to form these vessel-like structures, a process termed vasculogenic mimicry (16). In our nude mouse model of metastasis, both RL95 and HEC1A endometrial carcinoma cells that express Mig-7 localize to vessel-like structures formed by these invasive tumor cells (3). Adhesion assays to various components of the extracellular matrix (ECM) suggest that a mechanism for Mig-7 in vessel formation by tumor cells is due, at least in part, to significantly lower adhesion to laminins, probably through facilitating cleavage of laminin 5 γ2 chain (3). Membrane tethered metalloproteinase, MT1-MMP, cleaves laminin 5, and is required for invasion, metastases, and tumor growth in ECM (17–19). These studies led us to hypothesize that targeting Mig-7 by multiple methods would decrease invasion, enhance immune cell killing of tumor cells, and inhibit disease progression.

As an extension of previous Mig-7 cancer specificity studies, the present work shows that Mig-7 expression was detected in tumor cells of breast carcinoma and a subset of precancerous breast samples but not in cells of normal breast tissue samples. Several experimental systems were used to show, as proof-of-concept, that Mig-7 can be targeted. First, treatment with peptides specific to Mig-7 increased monocyte expression of tumor necrosis factor (TNF) and killing of breast carcinoma cells *in vitro*. Second, targeting Mig-7 with an antibody to its first nine amino acids reproducibly and significantly inhibited endometrial carcinoma cell invasion *in vitro*. Third, *in vivo* studies showed that shRNA decreased Mig-7 expression significantly impaired early tumor growth in an endometrial carcinoma cell xenograft nude mouse model. Active states of MT1-MMP (also known as MMP-14), ERK1/2, Akt, and S6 kinase were all reduced with Mig-7 targeting.

Materials and Methods

Cell Cultures and Transfections

Methods for constructing expression vectors, FLAGMig-7 and shRNA, as well as transfecting, selecting, and culturing HT29 colon carcinoma, HEC1A, RL95 endometrial carcinoma (2, 3, 20), and MCF-7 breast carcinoma (21) cell lines were previously described. Mig-7 sequence (Accession DQ080207) of the previously unpublished shRNA construct insert, 4-2 *antisense*-loop-*sense*, is *TCATTCACCTGCTATA-GACTTCAAGAGAGTCTATAGCAGG-TGAATGA* (bp 1303–1321). Under Institutional Review Board approval, human monocyte cells (MC) from breast adenocarcinoma

patients were isolated and cultured at 2×10^6 cells/mL in AIM-V^R serum-free lymphocyte medium (Life Technologies, Invitrogen) as previously described (21).

Modified Boyden Chamber Invasion Assay

Chemoinvasion assays were done as previously described (22). Briefly, transwell filters (8 μm; Costar) were blocked in 1% bovine serum albumin–DMEM/F12 for 30 min and rinsed with PBS. Matrigel (BD Biosciences) was diluted in ice-cold PBS to 1 mg/mL to coat the lower side of each transwell insert. After incubating at 37°C for 1 h, inserts were washed with PBS containing Ca^{2+} and Mg^{2+}. HEC1A cells were detached using trypsin without EDTA, neutralized with soybean trypsin inhibitor, centrifuged for 5 min at 1,000 rpm (4°C), and washed once in DMEM/F12 media. Cell count and viability were determined using trypan blue exclusion and a hemocytometer. HEC1A cells were preincubated with 10 μg/mL affinity-purified anti–Mig-7 peptide (first nine amino acids) rabbit polyclonal antibody (3, 4) or control normal rabbit IgG antibody (23) for 15 min in a 37°C, humidified incubator. For HEC1A cells, media containing 20 ng/mL of the chemoattractant, hepatocyte growth factor (HGF; R&D Systems, Inc.), was added to bottom wells. Medium without HGF containing 50,000 cells was added to each top well. Cells were allowed to invade for 24 h (HT29) or 72 h (HEC1A) at 37°C in 5% CO_2, 95% air humidified incubator. Then filters were rinsed with PBS and fixed in Hema3 fixative (Fisher Scientific, Inc.) for at least 30 min. Noninvaded cells in the upper chamber were removed with a cotton swab. Filters were dried and stained with Hema3 (Fisher Diagnostics) according to manufacturer's instructions. Filters were mounted on slides with gridded coverslips to count invaded cells using a microscope (Electron Microscopy Science) at ×400 magnification with a count of 10 squares (0.6 × 0.6 mm each) per filter from each treatment. Total numbers of invaded HT29 cells were counted and for HEC1A, percent invasion was calculated by extrapolating the average cell count for the entire filter surface area and dividing by initial cell number. No cells were observed in bottom wells that could have invaded through the Matrigel. All treatments were done in triplicate and experiments were repeated thrice.

Apoptosis Assay

Apoptosis was assessed using the Vybrant Apoptosis Assay kit #4 (Molecular Probes). For RL95 shRNA-expressing cell lines, 1×10^6 cells were plated in triplicate on six-well ultralow attachment plates (Corning, Inc.) for 18 h before analysis. For HEC1A cells, 1×10^6 cells were plated in 24-well plates and treated with Mig-7 antibody or rabbit IgG (10 μg/mL each) for 72 h before analysis. Cells were trypsinized and centrifuged to pellet followed by washing once in PBS. After suspending in 250 μL of PBS, cells were transferred to 96-well plates. One microliter of a 1:4 dilution of both YO-PRO-1 (100 μmol/L) and propidium iodide (PI; 1 mg/mL) was added to cells and incubated on ice for 30 min. Cells left unstained, or stained with YO-PRO-1 or PI alone, were also included for controls. Listmode data were collected using a FACSCalibur (Becton Dickinson) flow

cytometer and Winlist analysis software (Verity Software). Single-stained samples were used to perform compensation. Cells were gated to exclude large cell clumps and very small debris. YO-PRO-1–positive staining indicated apoptotic cells. YO-PRO-1 and PI double staining indicated dead cells. All cell lines or treatments were analyzed in triplicate and the experiments were done twice with similar results.

Proliferation Assay

Cell proliferation was assessed by using PI nuclear staining dye and flow cytometry as previously described (24). HEC1A cells were counted and 5×10^5 cells were plated in a 24-well plate and treated with IgG or Mig-7 antibodies as indicated above. For RL95 shRNA-expressing cell lines, 5×10^5 cells were plated and grown for 2 d before collection. All cells were fixed in 1 mL of 70% ethanol overnight. After fixation, cells were centrifuged ($470 \times g$, 5 min, 4°C) and the pellets washed once in 1× staining buffer (Dulbecco's PBS containing 2% FBS and 0.01% NaN_3). Cells were then treated with 1 mg/mL RNase A (Sigma) in PBS at 37°C for 30 min. After removing the RNase A solution, 300 μL of staining buffer containing 20 μg PI was added to resuspended cells and incubated 30 min at room temperature. PI was not added to one sample as a negative control. After 30 min, PI staining was analyzed using the FACSCalibur (Becton Dickinson). Levels of PI staining correlated to the different cell cycle phases, and the numbers of cells in the G_2-M phase (highest PI) were compared as an indicator of proliferation. Cells were gated to exclude large cell clumps and small debris. All cell lines or treatments were analyzed in triplicate and the experiments were done twice with similar results.

α2-Macroglobulin Capture Assay

This assay was done as previously described (25). Briefly, indicated cell lines were plated at confluency and treated as indicated in a six-well plate on 1 mg/mL Matrigel for 18 to 20 h before the assay. Cells were then removed by scraping and each sample was split into two wells of a 24-well plate. Purified human α2-macroglobulin (MP Biomedicals) was added to one of the two wells for each sample at a concentration of 1 mg/mL and incubated at room temperature for 15 min. Cells without α2-macroglobulin served as control. Following incubation, lysis buffer [2% SDS, 60 mmol/L Tris (pH 6.8), 10% glycerol and 2× protease inhibitors (Complete, Roche)] was added, at a 1:2 final dilution, and immunoblots done as detailed below. Assays were done in triplicate for each cell line and treatment. Lysates from cells without α2-macroglobulin treatment were pooled for immunoblot analyses. Individual density background levels for each lane were subtracted from the band of interest density level then divided by respective tubulin band density level for densitometry calculations.

Protein Phosphorylation Analyses

For protein phosphorylation analyses, confluent RL95 shRNA–expressing cells were plated on a 1:10 dilution of Matrigel (10.5 mg/mL) for 19 h before harvest. Confluent cells were trypsinized, pelleted at 4°C at 1,000 rpm for 4 min and washed thrice in media, followed by three washes in cold TBS. Multiprotein phosphorylation analysis using antibodies and Luminex Bead–based immunoassays was done by AssayGate, Inc. Briefly, indicated proteins in each cell lysate were determined quantitatively and simultaneously with a Bio-Plex 200 Bead Reader System. Antibodies were labeled with differing concentrations of two fluorophores to generate distinct bead sets. Each bead set was coated with capture antibody specific for each indicated total or phospho-protein. Captured analyte was detected using a biotinylated detection antibody and streptavidin-phycoerythrin. Analyses were done using a dual laser, flow-based, sorting and detection platform. One laser was bead-specific and determined a given antibody bound to protein. The other laser determined the magnitude of PE-derived signal, which is in direct proportion to the amount of protein bound. Protein concentrations of samples were determined by five-parameter logistic regression algorithm with analysis of the median fluorescence intensity readings of an eight-point protein standard curve. Once a regression equation was derived, the fluorescence intensity values of the standards were treated as unknowns and the concentration of each standard was calculated. A ratio of the calculated value to the expected value of this standard was determined. A ratio between 70% and 130% for each of the standards indicated a good fit. Precision was evaluated by the coefficient of variation, which equals the SD divided by the mean. All samples indicated a good level of precision.

Antibodies to phosphorylation sites analyzed included Ser^{473} for Akt, Thr^{202}/Tyr^{204} and Thr^{185}/Tyr^{187} for extracellular signal-regulated kinase 1/2 (ERK1/2), Thr^{246} for proline-rich Akt substrate of 40 kDa (PRAS40), Thr^{421}/Ser^{424} for S6 kinase, and Tyr^{1135}/Tyr^{1136} for insulin-like growth factor I receptor (IGF-IR). Antibodies to each protein were also used to detect total protein levels. Samples were tested in triplicate.

Immunoblotting

Cell lysates and immunoblots were done as previously described (2, 3) with the following modifications. Cultured cells were lysed in 2% SDS, 60 mmol/L Tris, and 10% glycerol containing 2× protease inhibitors (Complete, Roche) and quantitated using RC/DC Protein Assay (Bio-Rad). Lysates were boiled for 5 min in the presence of 100 mmol/L DTT and 0.01% bromophenol blue. Equal amounts of protein were loaded onto a 12% polyacrylamide gel and run at constant 200 V for 30 to 40 min. Gels were semidry transferred to polyvinylidene fluoride membranes and blocked in TBS-Tween (0.05%) containing 5% dry milk for 1 h at room temperature. Endogenous Mig-7 protein was detected using previously described affinity-purified Mig-7 antibody (3) at 0.16 μg/mL in TBS-T. After extensive washings, horseradish peroxidase (HRP)–labeled secondary anti-rabbit IgG antibody (Zymed Laboratories) was used to detect the Mig-7 antibody at 0.038 μg/mL in TBS-T. Mouse anti–β-tubulin (clone AA2; Upstate, Inc.) was used at 0.2 μg/mL in TBS-T followed by extensive washing and incubation with HRP-labeled secondary anti-mouse IgG

antibody (Cell Signaling). After stringent washings, Chemiluminescence Reagent (Amersham) allowed detection of HRP-labeled antibodies when exposed to film.

For α2-macroglobulin assay blots, lysates were not reduced or boiled before electrophoresis and transferring to nitrocellulose membrane. MT1-MMP (MMP-14) was detected using a goat anti-human MMP-14 antibody (R&D Systems, Inc.) at 0.1 μg/mL and an HRP-labeled secondary anti-goat IgG antibody (Zymed Laboratories) at 0.038 μg/mL.

Xenograft Nude Mouse Studies

Nude mouse studies were done under Institutional Animal Care and Use Committee approval as previously described with modifications (3, 4). Briefly, RL95 parental cells and cells stably transfected with shRNA expression vectors containing Mig-7–specific sequences 1-3, 3-1, or 4-2 G418 selected pooled colonies were described previously (2, 3). Cells were lifted off the plate using 1× trypsin-EDTA (Life Technologies, Invitrogen), followed by inhibition of trypsin using Defined Trypsin Inhibitor (Cascade Biologics). Viable cells were counted using trypan blue exclusion and a hemocytometer. For each injection, shRNA 1-3, 3-1, or 4-2–expressing RL95 cell lines were suspended at 5×10^5 each in serum-containing media with 10 ng/mL EGF (Life Technologies, Invitrogen) and 1:2 diluted Matrigel (10.3 mg/mL; BD Biosciences) and injected s.c. into the dorsal neck region of nu/nu athymic mice (National Cancer Institute). Negative controls were mice injected with Matrigel alone (no cells) and shRNA 3-1 RL95 cells that express Mig-7 at parental levels. Five animals were injected per cell line. Tumor size was measured with a caliper every 2 to 3 d and volume was calculated using (length × width^2)/2 as previously described (26). Mice were euthanized after 4 wk.

Immunohistochemistry

Breast core punch biopsies (10% formalin fixed, paraffin embedded, 5 μm) on tissue array slides were obtained from Cybrdi, Inc. Detection of Mig-7 protein was done using Mig-7–specific affinity-purified antibody as previously described (3, 4). Briefly, after deparaffinization and rehydration, antigen retrieval was done for 2 s on ice in a microwave oven. Slides were washed twice in Dulbecco PBS and then permeabilized with 0.01% digitonin (Sigma-Aldrich) in PBS at room temperature for 30 min. After washing twice in PBS, slides were blocked in 10% horse serum (Life Technologies, Invitrogen) in Dulbecco PBS for 30 min at room temperature. Affinity-purified, polyclonal, rabbit anti-peptide (first nine amino acids of Mig-7) primary antibody (0.32 μg/μL) was diluted 1:50 and incubated on the tissue sections overnight at 4°C. Slides were washed twice in PBS then incubated for 20 min in 3% H_2O_2 in methanol. After washing twice in PBS, slides were incubated for 30 min with secondary antibody, goat anti-rabbit IgG coupled to HRP, in PBS containing 0.5% bovine serum albumin (Fisher Scientific). Slides were washed twice in PBS and then developed using 3,3'-diaminobenzidine substrate (Vector Laboratories) until brown specific staining was detected by microscopy (<3 min). After washing in water for 5 min,

slides were counterstained in Hematoxylin QS (Vector Laboratories). Slides were dehydrated in 75%, 95%, and absolute ethanol, air dried, and coverslips mounted with DPX (BDH Laboratory Supplies). Secondary antibody alone or normal rabbit IgG instead of Mig-7 antibody served as controls.

Images were taken on a Nikon Microphot microscope with a Retiga 2000R digital CCD camera.

RNA Isolation and Reverse Transcription-PCR

Total RNA from normal breast tissue and from breast carcinoma cell lines were purchased from Ambion, Inc. Isolation of total RNA from MCF-7 breast carcinoma cells, DNasing, and reverse transcription-PCR (RT-PCR) was done as previously described (2–4).

Peptides

Control (MAA SRC SGL YIV RND TSG; YIV RND TSG LSG SQW VDS; LSG SQW VDS PLK SPC QVW) and Mig-7 (RVH MRA CSA GSA YLK QMK; GSA YLK QMK FCR MAA SLD; FCR MAA SLD KVK KTD RGE RG) peptides (Accession DQ080207) were synthesized by Biosource, Inc. Previously characterized MUC-1 peptide (GNN APA HGV NNA PDN RPA P; ref. 21) was synthesized by American Peptide Co., Inc. Peptides, 95% pure, were evaluated by mass spectrometry and solubilized in media.

### Stimulation of Human MCs and MCF-7 Killing Assays

Stimulations were done as previously described (21). Briefly, interleukin (IL)-2 (Cetus, Inc.) was added to isolated MC (see cell cultures) twice per week at 100 IU/mL on days 0 and 4. Cells were stimulated with 1 μg/mL of indicated peptides on days 0 and 7. MCF-7 cells (5×10^3 per well) were plated into 96-well tissue culture plates. Peptide-stimulated MC/effectors were added to each well in two effector cell to target cell ratios 10:1 and 5:1. Cell lysis was evaluated on day 8 of peptide stimulation using a tetrazolium salt XTT assay (Roche, Inc.) as previously described (27). Treatments were in replicates of six and each experiment was done at least twice.

Formation of formazan in XTT assays indicates viable cells. Formazan formed by target (MCF-7 cells) alone, MC/effector MC alone, or background (no cells) was determined as the mean of six wells each. The percent-specific lysis was calculated as previously described (21):

$$\%SL = \frac{OD_{(target-medium)} - OD_{(experimental\ wells-well\ with\ corresponding\ number\ of\ effector)}}{OD_{(target-medium)}} \times 100$$

ELISA Cytokine Assay

TNF-α concentration in media from each peptide-treated MC culture were determined using the human BD OptEIA cytokine assay that is a solid phase sandwich ELISA, according to manufacturer's instructions. Briefly, stimulated monocyte culture supernatant was added to TNF-α antibody–coated wells and incubated for 2 h. After washing, captured TNF was detected with a streptavidin-HRP–conjugate mixed with a biotinylated anti-human TNF-α antibody. After washing, 3,3',5,5'-tetramethylbenzidine substrate was added and the reaction was stopped after development.
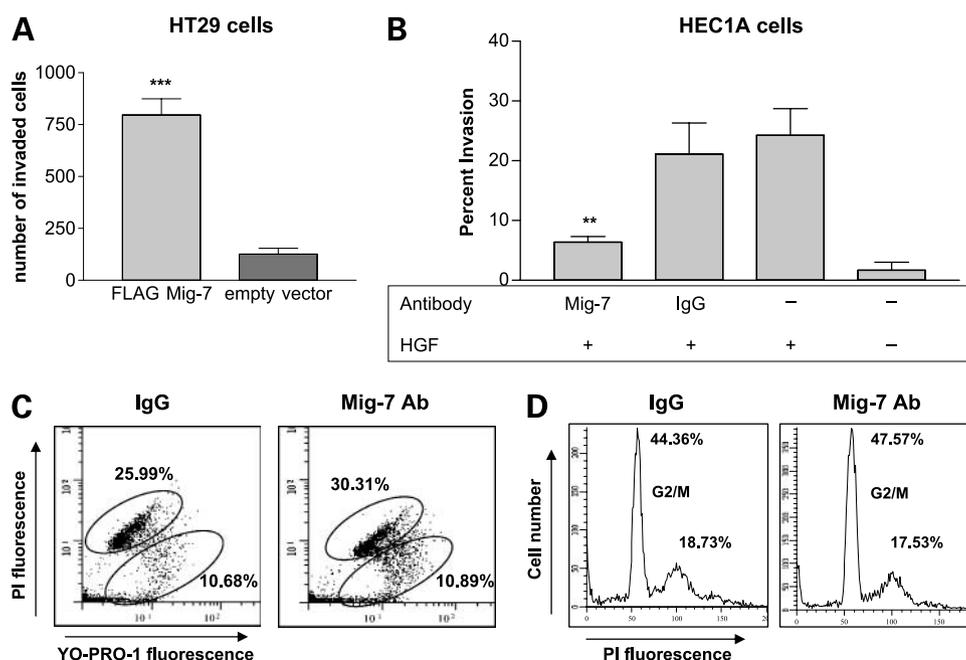
Figure 1. Mig-7–specific antibody decreases HEC1A endometrial carcinoma cell chemoinvasion. **A,** overexpression of amino terminus FLAG-tagged Mig-7 significantly increased Matrigel invasion of HT29 cells compared with vector alone stably transfected cells. *Columns,* mean; *bars,* SE. Results are after 24 h of invasion done in quadruplicate. **B,** Mig-7 affinity–purified antibody, but not IgG rabbit isotype antibody, significantly decreased chemoinvasion of HEC1A cells into Matrigel toward HGF ($P < 0.01$). *Ab,* antibody; + *HGF,* bottom wells contained 20 ng/mL HGF. Results shown are after 72 h of invasion and are representative of three independent experiments done in triplicate. *Columns,* mean; *bars,* SE. **C,** representative flow cytometry histograms of control normal rabbit IgG and Mig-7 antibody–treated HEC1A cells stained with YO-PRO-1 and PI. YO-PRO-1 single-positive cells (*bottom oval*) are apoptotic, and double-positive cells (*top oval*) are dead. Mean percentages of three samples are shown. **D,** representative flow cytometry histograms of control IgG and Mig-7 antibody-treated HEC1A cells stained with PI. Cells in G_2-M phase are indicated on histograms. Mean percentages of three samples are shown. Flow cytometry experiments were conducted twice with similar results.

Amounts of TNF-α were determined by measuring absorbance at 450 nm and comparison with a standard curve. The background of empty wells was subtracted before statistical analyses. Experiments were done in replicates of six for each peptide treated monocyte experiment.

Statistical Analysis

Statistical significance of the *in vitro* cytotoxicity assays and of cytokine assays were determined by the Mann-Whitney Rank Sum test. Data from HEC1A invasion assays and nude mouse xenograft assays were statistically analyzed by One-Way ANOVA and Tukey-Kramer posttest and considered significant at a P value of ≤ 0.05. Data from HT29 invasion assays, signaling phosphorylation studies, and α2-macroglobulin capture by MT1-MMP densitometry analyses were evaluated by a paired t test and considered significant at a P value of <0.05.

Results

Antibody to Mig-7 Treatment of HEC1A Cells Results in Decreased Invasion *In vitro*

A method to quantitatively assess tumor cell invasion is the transwell chemoinvasion assay (22). The effect of amino terminus FLAG-tagged Mig-7 (FLAGMig-7) overexpression in stably transfected HT29 colon carcinoma cells was quantitatively analyzed compared with vector alone–transfected cells. We chose this cell line because it does not endogenously express Mig-7 and it stably overexpresses FLAGMig-7 at the protein level (2, 3, 20). Overexpression in HT29 cells significantly increased the total number of invaded cells by 8-fold ($P = 0.002$) over control (Fig. 1A).

HGF, the growth factor used to isolate Mig-7 (2), acts as a chemoattractant of invasive HEC1A cells in transwell *in vitro* assays (28). Therefore, we used this cell line, previously shown to express Mig-7 (2, 3), treated with affinity-purified antibody to Mig-7 peptide representing its first nine amino acids to determine if this antibody could inhibit cell invasion.

Mig-7 antibody treatment of HEC1A cells significantly decreased the average percentage of invaded cells counted as described in Materials and Methods. Chemoinvasion toward HGF by HEC1A cells was significantly ($P = 0.0046$) inhibited by 70% when treated with Mig-7 antibody and compared with normal rabbit IgG antibody–treated cells (Fig. 1B). Furthermore, treatment with normal rabbit IgG antibody did not significantly inhibit HEC1A cell chemoinvasion when compared with no antibody treatment. No HGF chemoattractant reduced invasion of HEC1A cells by >90% (Fig. 1B). Flow cytometric analysis with the apoptotic dye YO-PRO-1 and PI showed no significant increase in apoptosis due to Mig-7 antibody compared with normal rabbit IgG antibody treatment (Fig. 1C). In

addition, flow cytometric cell cycle analysis showed no significant decrease in cell proliferation of Mig-7 antibody–treated cells compared with untreated and control-treated cells (Fig. 1D).

Antibody or Expression of shRNA Specific to Mig-7 Decreases Activity of MT1-MMP

MT1-MMP activity is required for tumor cell invasion (17, 18) and Mig-7 expression significantly increases this invasion (2, 3). Mig-7 protein is primarily membrane localized and is cysteine rich (1). A free thiol group on one of the many cysteine residues in membrane-localized Mig-7 could activate MT1-MMP without cleavage via the "cysteine switch" (29, 30). Therefore, we used the α2-macroglobulin capture assay to test for MT1-MMP activation. In addition, this test was used instead of zymography because the SDS in gel zymography activates the cysteine switch (31).

HEC1A cells treated with Mig-7 antibody showed a significant 70% decrease in the levels of activated MT1-MMP, as indicated by the upper, α2 macroglobulin captured band (~190 kDa), compared with cells treated with IgG control. The lower uncaptured, unactivated MT1-MMP band was 62 kDa as indicated. Levels of activated MT1-MMP were determined by densitometry normalized with tubulin levels for each sample (Fig. 2A).

Given that Mig-7 antibody treatment reduced levels of active MT1-MMP, we next tested whether stable knockdown of Mig-7 expression in RL95 cells could inhibit MT1-MMP

activation. In this study, we used previously characterized RL95 endometrial carcinoma cells stably expressing shRNA constructs 1-3 and 3-1. In that study, the 1-3 construct expression significantly inhibits Mig-7 protein levels by at least 50% compared with the 3-1 control construct expression that does not significantly reduce the Mig-7 protein levels (3). In Fig. 2B, α2-macroglobulin capture assays revealed that 1-3 shRNA RL95 cells decreased levels of active MT1-MMP by 57% compared with control (2). Analysis of these cell lines by flow cytometry for apoptosis and proliferation showed no significant differences between 1-3 and control cell lines (Fig. 2C and D).

Expression of shRNA Specific to Mig-7 Decreases Phosphorylation of ERK1/2, Akt, and S6 Kinase

To further define potential mechanisms by which Mig-7 exerts its effects on invasion, a multiplex protein phosphorylation analysis was used to determine changes in protein activation. Phosphorylation status of proline-rich Akt substrate of 40 kDa (PRAS40), ribosomal protein S6 kinase, extracellular signal-regulated kinase1/2 (ERK1/2), IGF-IR, and Akt (also known as protein kinase B) were analyzed as described in Materials and Methods. In cell lysates from RL95 cells with decreased Mig-7 protein levels due to stable shRNA 1-3 expression (2), phosphorylation of Akt Ser^{473}, ERK1/2 Thr^{202}/Tyr^{204}, Thr^{185}/Tyr^{187}, and S6 kinase Thr^{421}/Ser^{424} were significantly reduced by 10%, 40%, and 30%, respectively, compared with control (Fig. 3A). No
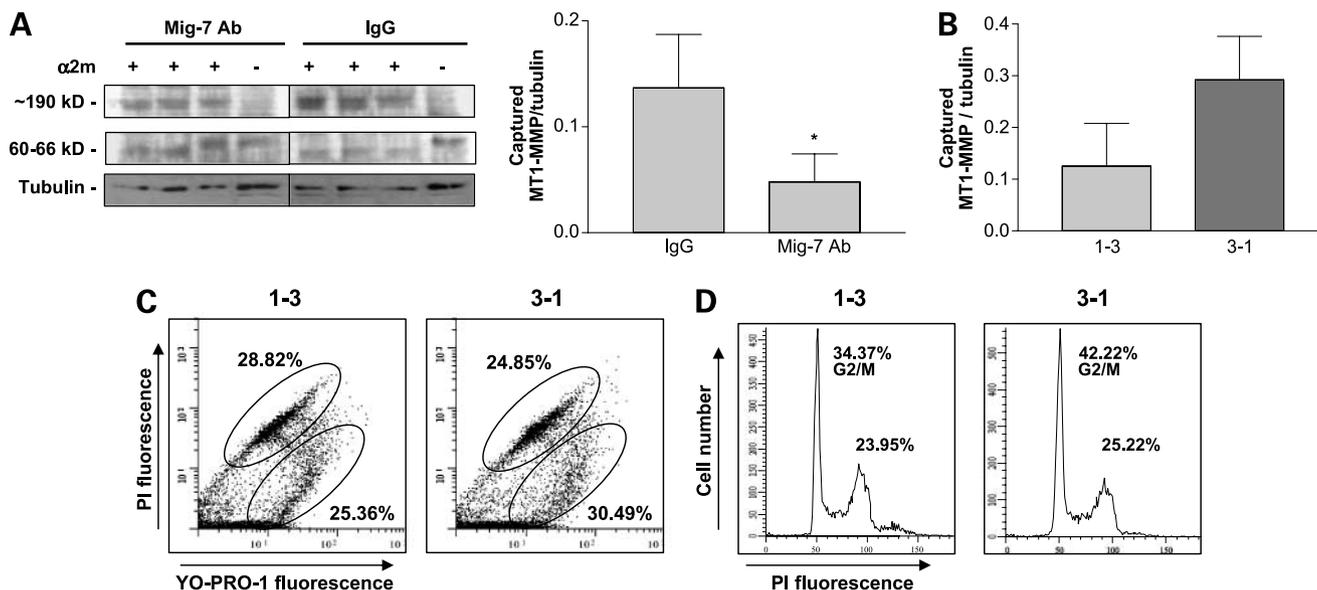
Figure 2. Antibody or expression of shRNA specific to Mig-7 decreases activity of MT1-MMP. **A,** representative immunoblot and densitometry results for α2-macroglobulin capture assay of active MT1-MMP in lysates from equal numbers of HEC1A cells treated with normal rabbit IgG or with Mig-7 antibody. All samples were run on the same gel. Mig-7 antibody treatment significantly decreased MT1-MMP activity by 70% compared with IgG treatment ($P = 0.0496$). Densitometry data are for the upper, captured MT1-MMP band in each lane normalized to its respective tubulin band. *Columns,* mean; *bars,* SE. **B,** densitometry analysis of the upper, captured MT1-MMP band from α2-macroglobulin capture assay in lysates from RL95 cells stably transfected with shRNA 1-3 (decreased Mig-7 expression) and 3-1 (control, endogenous levels of Mig-7 expression). Results are normalized to β-tubulin. RL95 cells expressing shRNA 1-3 showed a 57% decrease in MT1-MMP activity compared with 3-1 control cells. *Columns,* mean; *bars,* SE. **C,** representative flow cytometry histograms of RL95 shRNA 1-3 and 3-1 stably transfected cells stained with YO-PRO-1 and PI. YO-PRO-1 single-positive cells (*bottom oval*) were apoptotic, and double-positive cells (*top oval*) were dead. Mean percentages of three samples are shown. **D,** representative flow cytometry histograms of RL95 shRNA 1-3 and 3-1 stably transfected cells stained with PI for cell cycle analysis. Cells in G_2-M phase are indicated on histograms. Mean percentages of three samples are shown. Flow cytometry experiments were conducted twice with similar results.
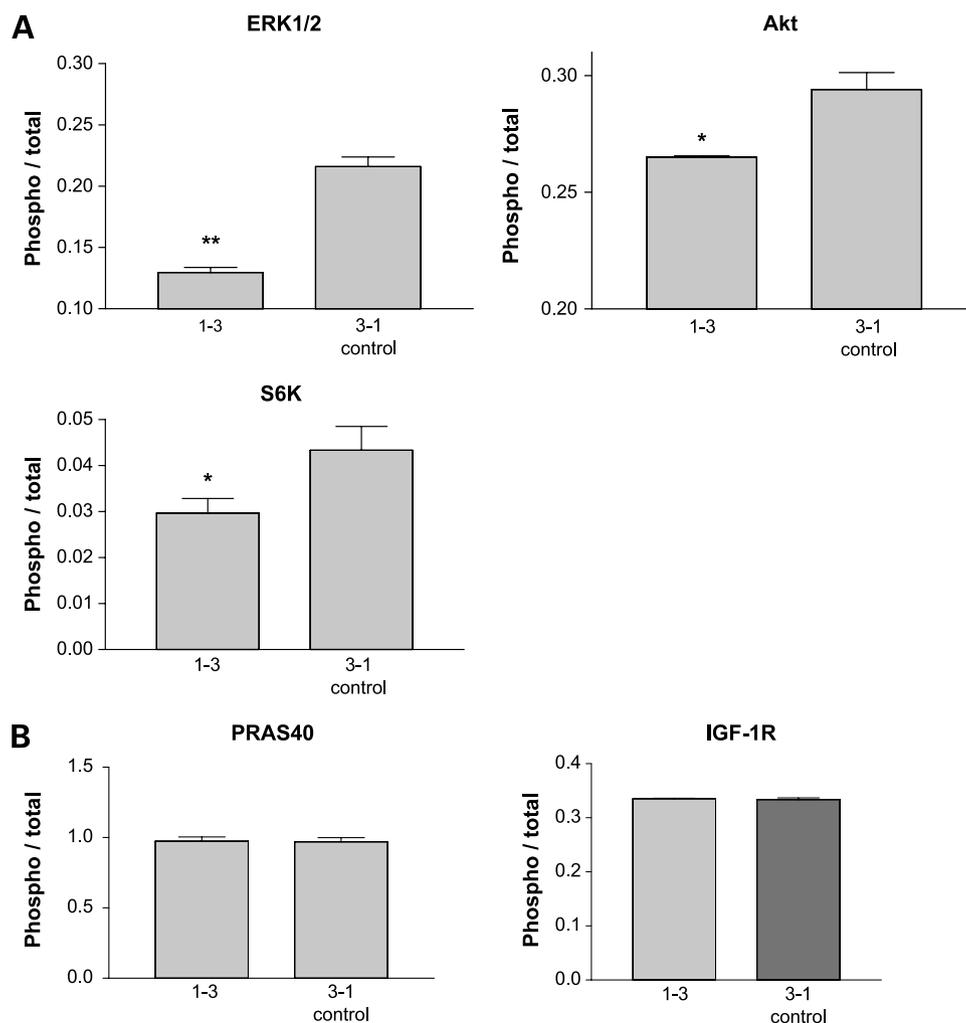
Figure 3. Expression of shRNA specific to Mig-7 decreases S6 kinase, ERK1/2, and Akt phosphorylation in RL95 cells. **A,** normalized fluorescence intensity from analysis of phosphorylated ERK1/2, Akt, and S6 kinase in RL95 shRNA 1-3 (knockdown) and 3-1 (control) stably transfected cells. Cells were plated and prepared as given in Materials and Methods. 1-3 shRNA–expressing cells, in which levels of Mig-7 are significantly reduced by >50% (2), showed significant phosphorylation decreases in ERK1/2 by 40% ($P = 0.002$), in Akt by 10% ($P = 0.0449$), and in S6 kinase by 30% ($P = 0.0155$) compared with control RL95 cells that express levels of Mig-7 similar to the RL95 parental cell line. **B,** normalized fluorescence intensities from analysis of phosphorylated PRAS40 and IGF-IR. All phosphorylation fluorescence intensities were normalized to total respective protein fluorescence intensities. These experiments were done in triplicate.

significant differences in phosphorylation between these two RL95 cell lines were detected for PRAS40 or for IGF-IR (Fig. 3B).

Stimulation of Human Peripheral Blood Monocytes (MC) with Peptides Specific to Mig-7 Increases TNF Expression and Killing of MCF-7 Breast Carcinoma Cells *In vitro*

Cancer immunotherapies include *ex vivo* stimulation of cancer patients' immune cells with tumor antigens. We hypothesized that Mig-7 peptides could stimulate breast cancer patients' MC to increase their killing of breast carcinoma cells *in vitro*. To test this hypothesis, we utilized our previously described methods of MC, isolated from two different breast cancer patients, stimulated with indicated peptides and the MCF-7 breast carcinoma cell line (21, 32). Because

Mig-7 expression induces invasion (3), we wanted a cell line that lacks invasive properties to test if Mig-7 could still be used as a target in such a model cell line. The MCF-7 cell line is lowly invasive due to deficiency of MT1-MMP and MMP-2 (33). In addition, MCF-7 cells express $\alpha v\beta 5$ integrin (34, 35) that is required for Mig-7 expression (2). Furthermore, our use of MCF-7 cells in the current study was warranted by the fact that this experimental system is optimized with this cell line (21, 32), and that MCF-7 cells expressed Mig-7 mRNA and protein (Fig. 4A).

Mig-7 peptides representing the +1 frameshifted protein sequence or control peptides representing the sequence in the noncoding reading frame, i.e., the frame that did not produce protein (20), were used to stimulate MC *in vitro*. In addition, these peptides included overlapping sequences

(see Materials and Methods) to prevent the possible omission of an epitope. None of the peptides were significantly homologous to any other sequence than the Mig-7 banked sequence in databases available through the National Center for Biotechnology Information. MUC-1 peptide served as an internal control because of its previous use and optimization in this assay. These previous studies of stimulating MC cells with MUC-1 peptide and IL-2 support the presentation of peptide by antigen-presenting cells that stimulate CTL s in this heterogeneous cell population (21, 32).

Stimulation with Mig-7 peptides significantly enhanced MC/effector killing of MCF-7 cells by 3-fold over MUC-1 peptide alone (0) or control (*CTL*) peptides. There was no significant difference between control peptides and MUC-1 peptide alone treatment groups (Fig. 4B). Figure 4C shows that a ratio of 10:1 MC/effector/MCF-7 cells resulted in no difference between no peptide and MUC-1-stimulated MC/effector killing of MCF-7 cells. In contrast, at this ratio, Mig-7 with MUC-1 peptides significantly increased MC/effector killing of MCF-7 cells >2-fold over no peptide or MUC-1–stimulated cells. Also at this higher MC/effector cell ratio, IL-2, which enhances cytotoxic activity of T and natural killer cells (21, 36), treatment alone of MC/effectors

increased their level of killing to that detected for cells stimulated with IL-2 plus MUC-1 peptide. At a 5:1 ratio, Mig-7 with MUC-1 peptides stimulation of MC significantly enhanced their killing of MCF-7 cells 1.9-fold over MUC-1-peptide stimulation and at least 30-fold over no peptide stimulation (Fig. 4C). Mig-7 peptide stimulation also significantly increased levels of MC/effector-produced TNF-α >3-fold over control peptide-stimulated cells as determined by ELISA (Fig. 4D).

Mig-7 Expression Is Specific to Breast Carcinoma and Not to Normal Breast

To date, Mig-7 expression is detected in multiple types of tumor cells, but not in normal cells (2–4). However, normal breast cells were absent in our previous studies. Here, we extend our analyses of Mig-7 specificity with analyses of cells in breast tissues of precancerous states and carcinomas compared with normal breast tissues. First, relative RT-PCR was used as previously described (2–4) to analyze commercially available total RNA from three breast carcinoma cell lines, T47D, MDA-MB453, DU4475, and from normal breast tissue from three subjects with no previous history of cancer. No amplification product specific to Mig-7 was detected in normal breast tissue RNA samples. However, all
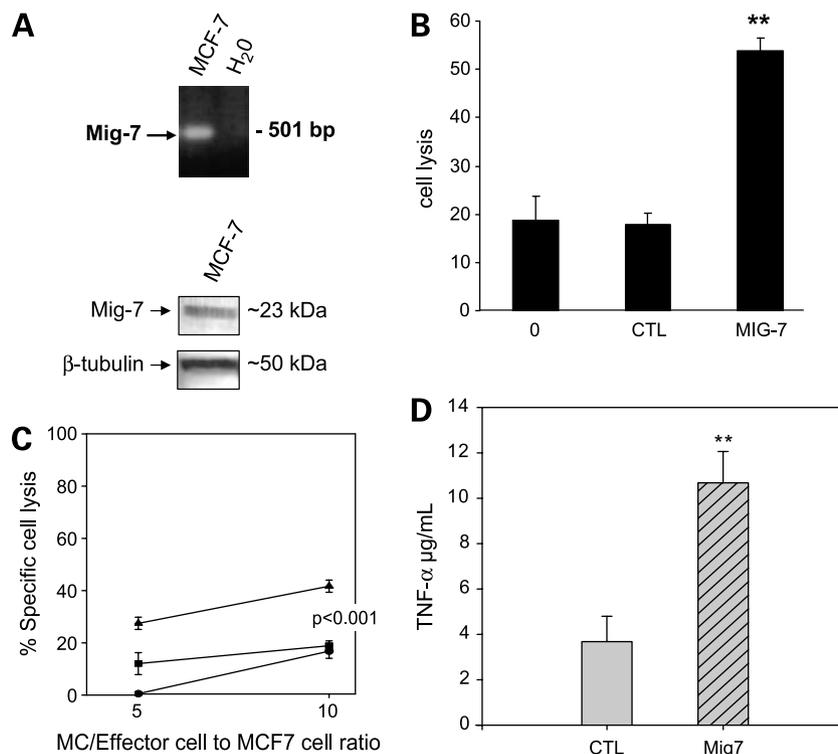
Figure 4. Mig-7 peptides enhance human monocyte killing of MCF-7 breast carcinoma cells. **A,** MCF-7 cells expressed Mig-7 mRNA by RT-PCR and protein by immunoblot analyses. Experiments were repeated twice. **B,** human MC cells stimulated with IL-2 and either MUC-1 peptide (0), pooled control peptides (*CTL*), or pooled Mig-7 peptides (sequences given in Materials and Methods). MC/effector cell lysis of MCF-7 cells as described in Materials and Methods. Note that Mig-7 peptides significantly ($P < 0.001$) enhanced MC/effector killing of MCF-7 carcinoma cells. Experiments have been repeated thrice in replicates of six for each treatment group. MCs were isolated from two different individuals. **C,** MC after stimulations to effector cells ratio to MCF-7 cells and respective percentages of MCF-7 cell–specific lysis. ———●———, no peptide; ———■———, MUC-1 peptide; ———▲———, MUC-1 plus Mig-7 peptides treatment groups. *Columns,* mean; *bars,* SE. Experiments were repeated twice with replicates of six for each treatment group. **D,** TNF-α production by human isolated MC after indicated peptide stimulation. TNF-α production was measured by ELISA assay as described in Materials and Methods after MC were cultured for 8 d with control peptides or with Mig-7 peptides. Assays were done in replicates of six in three independent experiments with identical results.

A

501 bp — Mig-7

324 bp — 18s

ladder T-47D MDA-MB453 DU4475 normal

B

C

D
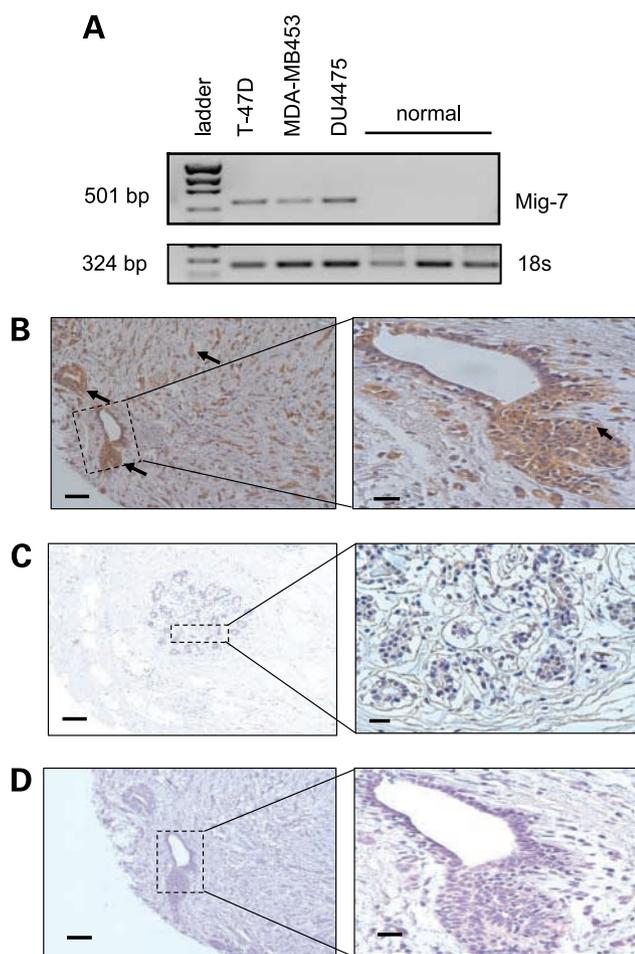
Figure 5. Mig-7 expression is specific to breast carcinoma tissue and cell lines. **A,** representative Mig-7–specific relative RT-PCR of three breast carcinoma cell lines (T47D, MDA-MB453, DU4475) and commercially available RNA from normal breast tissue of three different human subjects without previous histories of cancer. **B** to **D,** representative images of Mig-7 antibody immunohistochemistry on breast tissue array from Cybrdi, Inc., as described in Materials and Methods. Core samples from (**B**) breast carcinoma. *Arrows,* positive Mig-7 staining. **C,** representative normal breast tissue immunohistochemistry with Mig-7 antibody, and (**D**) Representative image of control normal rabbit IgG instead of Mig-7 as primary antibody immunohistochemistry of breast carcinoma tissue section (serial section to that shown in **B**). Hematoxylin was used to counterstain. Note a lack of specific staining in **D** compared with **B**. Images were taken at ×100 magnification with inserts at ×400 magnification. *Scale bars,* 100 μm for ×100 images and 20 μm for inserts.

three breast carcinoma cell lines expressed Mig-7 mRNA (Fig. 5A).

Immunohistochemistry was done on 70 human breast tissue arrayed core samples of normal, adenosis, papillomatosis, and carcinoma. Our results showed that primarily carcinoma tissues (Fig. 5B) stained positive for Mig-7, whereas normal breast tissues lacked specific Mig-7 staining (Fig. 5C). No staining was detected with normal rabbit IgG antibody in breast carcinoma tissue serial section to that in Fig. 5B (Fig. 5D). A summary of the overall pathology report of Mig-7 staining for all 70 samples is as follows: normal: 0 positive, 3 negative; breast adenosis: 5 positive,

23 negative; breast papillomatosis: 0 positive, 3 negative; and breast carcinoma: 19 positive, 17 negative. Pearson χ^2 analysis with 3 degrees of freedom to test goodness of Mig-7 fit for detection of breast carcinoma was statistically significant ($P = 0.008$).

Stable Knockdown of Mig-7 Expression Reduces Early Primary Tumor Growth *In vivo*

Mig-7 induces HT29 colon carcinoma cell invasion in three-dimensional cultures (3) and MT1-MMP proteolysis enables tumor cells to circumvent three-dimensional ECM growth restraint (19). These data led us to test the effect of stable Mig-7 knockdown, through shRNA expression, on primary tumor growth *in vivo*.

Three RL95 endometrial carcinoma cell lines stably transfected with different Mig-7 shRNA-containing expression plasmids, 1-3, 4-2, and negative control 3-1 were each injected s.c. into nude mice and tumor growth measured as described in Materials and Methods. We confirmed our previous results (3) that cells expressing shRNA 1-3 have reduced Mig-7 protein levels compared with parental and 3-1-expressing cells by Western blot (Fig. 6A). 1-3 expressing cells showed an approximate 50% to 60% decreased Mig-7 protein levels compared with 3-1-expressing cells that in previous studies show levels of Mig-7 protein similar to parental RL95 cell line (2). In addition, expression of a previously unpublished Mig-7 shRNA construct, 4-2, reduced Mig-7 protein levels by amounts similar to 1-3–expressing cells (Fig. 6A).

Upon measuring (see Materials and Methods) primary tumors of all five mice for each cell line, RL95 cells expressing shRNA 1-3 and 4-2 showed significant ($P < 0.05$) decreased tumor volume, 60% and 40% to 50%, respectively, at 13 and 15 days after injection compared with mice injected with control cells expressing shRNA 3-1 (Fig. 6B). Although tumor volume trended lower for shRNA-expressing cells at days 18 and 23, this was not significantly different than control cell line growth (Fig. 6B). Mice injected with Matrigel alone showed no tumor formation across the entire time period (data not shown).

Discussion

Targeting Mig-7 protein with an antibody to its amino terminus, nine amino acids significantly decreased HEC1A endometrial carcinoma cell chemoinvasion and MT1-MMP activation. Compared with controls, stimulating breast cancer patients' isolated MC with Mig-7–specific peptides increased their killing of MCF-7 breast carcinoma cells as well as MC production of TNF-α *in vitro*. In addition, specific shRNA knockdown of Mig-7 protein levels in RL95 cells decreased MT1-MMP, ERK1/2, Akt, and S6 kinase active states *in vitro* as well as early tumor growth *in vivo*. These results are consistent with our previous reports that show Mig-7 contributes to the invasive phenotype of carcinoma cells (2, 3).

Immunohistochemical and RT-PCR data in the present study further show the specificity of Mig-7 expression to breast carcinoma tissue and not to normal breast tissues.

These data are not surprising because even with 40 cycles of PCR, Mig-7 mRNA is not detected in 25 different normal human tissues (*n* = 6 each tissue) or in blood from normal subjects (2, 4). This specificity of Mig-7 expression may be due to multiple tumor microenvironment factors such as ligation of αvβ5 integrin and multiple growth factors leading to Mig-7 transcription (2, 3) as well as multiple events required for Mig-7 translation (20). The percentage of total breast carcinoma tissues staining for Mig-7 was 53%. This result may be due to the fact that only a small core of each tumor tissue is represented on these tissue microarrays and the invasive front of carcinoma cells may not be represented in all of these core samples. Our previous data, however, show that 98% of cDNA from breast carcinoma tissue samples (*n* = 50) contain moderate to high levels of Mig-7 (4). Mig-7 is also expressed in a subset of human breast adenosis samples with hyperplasia, which is considered a "precancerous" tissue (37). A similar subset of precancerous endometrial lesions are positive for Mig-7 (4). These data

further support our previous findings (2, 4) that Mig-7 expression is specific to tumor cells and not found in normal adult cells.

Mig-7 antibody significantly inhibited invasion of endometrial carcinoma cells *in vitro*, suggesting that treatment with Mig-7 antibody *in vivo* may inhibit invasion. Previous studies show that antibody to CXCR4, a chemokine receptor, inhibits invasion of carcinoma cells (38). Further studies are needed to determine the effects of Mig-7–specific antibodies on tumor progression *in vivo*.

MT1-MMP activity causes activation of MMP-2 (gelatinase A; ref. 39), cleavage of laminin-5 (17), increased invasion (40), and is required for tumor cell vasculogenic mimicry (11). Thus, because Mig-7 expression significantly increases invasion, decreases adhesion to laminins, increases laminin 5 γ2 domain 3 fragmentation, and seems to play a role in vessel-like structure formation by endometrial carcinoma cells (3), we hypothesized that Mig-7 expression facilitates MT1-MMP activation. Data from the present studies show that inhibiting Mig-7 function by antibody treatment or expression by Mig-7 shRNA leads to decreased levels of activated MT1-MMP, suggesting a mechanism by which Mig-7 promotes the above cellular events. MT1-MMP can be activated through the cysteine switch mechanism (29, 30) and Mig-7 is highly cysteine rich (2, 20). Additional studies beyond the scope of this work are needed to determine if one or more Mig-7 cysteine residues play a role in MT1-MMP activation.

Consistent with Mig-7 facilitating activation of MT1-MMP and invasion are data showing that Mig-7 expression leads to increased levels of phosphorylated ERK1/2, Akt, and S6 kinase. MT1-MMP catalytic activity or binding to tissue inhibitor of metalloproteinases-2 without proteolytic activity induces ERK1/2 phosphorylation (41, 42). Other signaling molecules analyzed in the present study, IGF-IR and PRAS40, which are known to play roles in tumor progression (6, 43), showed no decrease in phosphorylation due to reduced Mig-7 protein levels, which further supports specific effects of Mig-7 expression on ERK1/2, Akt, and S6 kinase signaling molecules.

ERK1/2 and Akt phosphorylation signals invasion downstream of RTK activation and αv integrin ligation (44–46). RTK activation by epidermal growth factor or HGF in concert with αvβ5 ligation also induces Mig-7 expression (2, 3). Similarly, S6 kinase activation downstream of HGF, ERK1/2, and Akt signaling is important for tumor cell migration (47). Not surprisingly, activation of ERK1/2 and Akt downstream of RTK signaling facilitates MT1-MMP activation (48–50). Taken together, these data suggest that Mig-7 is an intermediate signaling protein downstream of RTK activation and αvβ5 integrin ligation (2), and upstream of MT1-MMP, ERK1/2, Akt as well as S6 kinase.

Enhanced killing of noninvasive, MT1-MMP–negative, Mig-7–expressing MCF-7 breast carcinoma cells by monocytes stimulated with IL-2 and Mig-7–specific peptides suggests that Mig-7 is a tumor cell antigen. In addition, these experiments show that Mig-7 peptides combined with MUC-1 peptides are superior in stimulating MC to
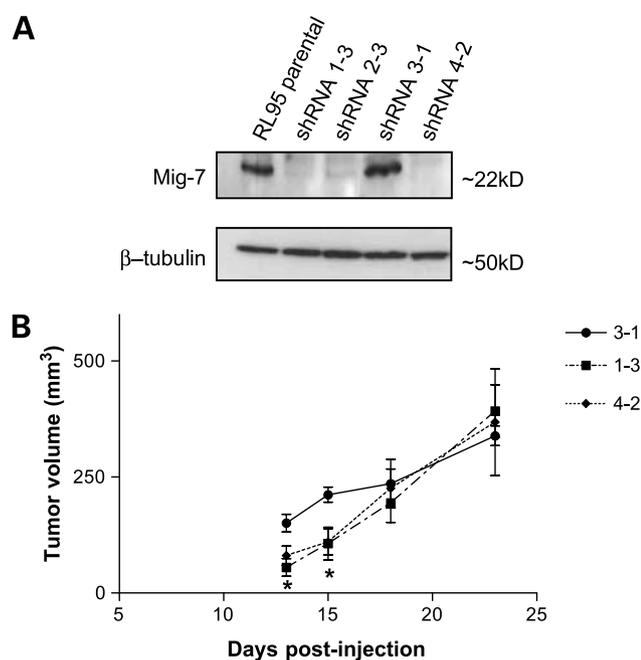
Figure 6. Stable knockdown of Mig-7 expression in RL95 cells decreases early primary tumor growth in nude mice. **A,** representative immunoblot of equal amounts of protein lysates from RL95 parental and Mig-7–specific shRNA stably transfected pooled clones 1-3, 3-1, and 4-2 cell lines. *Top,* after probing with Mig-7 antibody. Blot was reprobed with tubulin antibody to confirm equal loading and transfer. Statistical analyses of 1-3, 3-1, and parental Mig-7 knockdown and sequences of specific shRNAs were shown previously (2) and 4-2 levels of Mig7 protein were equivalent to those found in 1-3 shRNA knockdown of Mig-7 protein. See Materials and Methods for 4-2 shRNA sequence. **B,** representative graph showing tumor volumes (mm³) measured 13, 15, 18, and 23 d after injection of Matrigel containing RL95 cell lines stably transfected with shRNA constructs 1-3, 4-2, or 3-1 (control) into nude mice (five animals per cell line, as described in Materials and Methods). Note that cells expressing shRNAs 1-3 or 4-2, which significantly knockdown Mig-7 protein levels, showed significant 60% and 40% to 50% (*P* < 0.05) decreased tumor volume, respectively, at days 13 and 15 of tumor growth. *Points,* mean; *bars,* SE. Anova with Tukey's Multiple Comparison Test was used for statistical analyses. This experiment was done twice with similar results.

kill MCF-7 cells over MUC-1 peptide or control peptides. Furthermore, Mig-7 peptide stimulation of monocytes enhanced production of TNF-α, a cytokine known to cause tumor cell death (51). This is probably the mechanism of cell killing in our assay because MCF-7 cells are responsive to TNF-α (52). These data suggest that Mig-7 peptides could be used *ex vivo* to stimulate MC/effector cells and test their tumor cell killing *in vivo.*

Inhibition of Mig-7 expression by stable Mig-7–specific shRNA expression significantly reduced early tumor growth *in vivo*. With two different Mig-7 knockdown RL95 cell lines (1-3 and 4-2), significant 40% to 60% decreased tumor growth compared with control was measured at days 13 and 15 after injection. This result is likely due to decreased invasion and decreased MT1-MMP proteolytic activity from reduced Mig-7 expression. In support of this conclusion, MCF-7 cells expressing MT1-MMP with a mutation E240A rendering it proteolytically inactive produces tumors 50% the size of wild-type MT1-MMP (42). In our previous studies, HT29 colon carcinoma cells overexpressing FLAG-tagged Mig-7 or RL95 parental cells strictly invade Matrigel ECM during the first 10 days of three-dimensional culture (3). This probably also occurred with the current *in vivo* studies when RL95 cell lines were combined with Matrigel and injected s.c. We propose that the RL95 3-1 cell line, expressing parental levels of Mig-7 protein, efficiently invades the Matrigel, whereas knockdown cell lines (1-3 and 4-2) poorly invade the Matrigel *in vivo* as we have previously observed in Matrigel three-dimensional cultures (3). This lack of invasion could inhibit proliferation due to ECM constraint at least at these earlier time points.

MT1-MMP activity was reduced in 1-3–expressing RL95 cells compared with 3-1 cells that express Mig-7 protein at parental cell line levels. In another report, MT1-MMP confers SCC-1, Panc-1 and HT-1080 cell lines with a significant growth advantage in three-dimensional cultures *in vitro* and *in vivo* (19). This advantage requires MT1-MMP activity and proteolysis to release the constraints of the surrounding ECM (19). Primary tumor sizes in the present study were not significantly different at days 18 and 23 after injection. Consistent with these data, Mig-7 expression caused no difference in proliferation or apoptosis in these cell lines *in vitro* when plated on Matrigel. One explanation for these later *in vivo* time points is that MT1-MMP binds to tissue inhibitor of metalloproteinases-2 that induces mitogen-activated protein kinase and ERK1/2 activation as well as cell growth without proteolysis *in vivo* (42). Alternatively, Matrigel may not be stable at these later time points, and therefore, its constraint on proliferation may be absent. We propose that this may have occurred resulting in more rapid growth in the knockdown cell line tumors without invasion at these later time points.

Based on these data and because Mig-7 facilitates invasion in three-dimensional cultures (2), it is likely that reduction of Mig-7 expression in RL95 cells slows early primary tumor growth by inhibiting local tumor cell invasion in Matrigel. Different models of tumor growth and metastases, such as an orthotopic model, may provide additional information on how Mig-7 expression impacts disease progression. Future studies beyond the scope of this present work are required to determine if Mig-7 plays a role in MT1-MMP tyrosine573 phosphorylation that is required for this growth advantage in ECM (53) or if ERK1/2 phosphorylation is affected by Mig-7 activation of a nonproteolytic MT1-MMP (42) in the presence or absence of tissue inhibitor of metalloproteinases-2 at physiologic levels.

Disclosure of Potential Conflicts of Interest

No potential conflicts of interest were disclosed.

References

1. Condeelis J, Singer RH, Segall JE. The great escape: When cancer cells hijack the genes for chemotaxis and motility. Annu Rev Cell Dev Biol 2005;21:695–718.

2. Crouch S, Spidel CS, Lindsey JS. HGF and ligation of avb5 integrin induce a novel, cancer cell-specific gene expression required for cell scattering. Exp Cell Res 2004;292:274–87.

3. Petty AP, Garman KL, Winn VD, Spidel CM, Lindsey JS. Overexpression of carcinoma and embryonic cytotrophoblast cell-specific Mig-7 induces invasion and vessel-like structure formation. Am J Pathol 2007;170:1763–80.

4. Phillips TM, Lindsey JS. Carcinoma cell-specific Mig-7: a new potential marker for circulating and migrating cancer cells. Oncol Rep 2005;13:37–44.

5. Robertson GP. Mig-7 linked to vasculogenic mimicry. Am J Pathol 2007;170:1454–6.

6. Brooks PC, Klemke RL, Schon S, Lewis JM, Schwartz MA, Cheresh DA. Insulin-like growth factor receptor cooperates with integrin α v β 5 to promote tumor cell dissemination *in vivo*. J Clin Invest 1997;99:1390–8.

7. Klemke RL, Yebra M, Bayna EM, Cheresh DA. Receptor tyrosine kinase signaling required for integrin α v β 5-directed cell motility but not adhesion on vitronectin. J Cell Biol 1994;127:859–66.

8. Beard J. Embryological aspects and etiology of carcinoma. Lancet 1902;1:1758–61.

9. Red-Horse K, Zhou Y, Genbacev O, et al. Trophoblast differentiation during embryo implantation and formation of the maternal-fetal interface. J Clin Invest 2004;114:744–54.

10. Soundararajan R, Rao AJ. Trophoblast 'pseudo-tumorigenesis': significance and contributory factors. Reprod Biol Endocrinol 2004;2:15.

11. Seftor REB, Seftor EA, Koshikawa N, et al. Cooperative interactions of laminin 5 g2 chain, matrix metalloproteinase-2, and membrane type-1 matrix/metalloproteinase are required for mimicry of embryonic vasculogenesis by aggressive melanoma. Cancer Res 2001;61:6322–7.

12. Maniotis AJ, Folberg R, Hess A, et al. Vascular channel formation by human melanoma cells *in vivo* and *in vitro*: Vasculogenic mimicry. Am J Pathol 1999;155:739–52.

13. Sood AK, Seftor EA, Fletcher MS, et al. Molecular determinants of ovarian cancer plasticity. Am J Pathol 2001;158:1279–88.

14. Sun B, Zhang S, Zhang D, et al. Vasculogenic mimicry is associated with high tumor grade, invasion and metastasis, and short survival in patients with hepatocellular carcinoma. Oncol Rep 2006;16:693–8.

15. van der Schaft DWJ, Hillen F, Pauwels P, et al. Tumor cell plasticity in Ewing sarcoma, an alternative circulatory system stimulated by hypoxia. Cancer Res 2005;65:11520–8.

16. Hendrix MJC, Seftor EA, Kirschmann DA, Quaranta V, Seftor REB. Remodeling of the microenvironment by aggressive melanoma tumor cells. Ann NY Acad Sci 2003;995:151–61.

17. Koshikawa N, Minegishi T, Sharabi A, Quaranta V, Seiki M. Membrane-type matrix metalloproteinase-1 (MT1-MMP) is a processing enzyme for human laminin {γ}2 chain. J Biol Chem 2005;280:88–93.

18. Koshikawa N, Giannelli G, Cirulli V, Miyazaki K, Quaranta V. Role of cell surface metalloprotease MT1-MMP in epithelial cell migration over laminin-5. J Cell Biol 2000;148:615–24.

19. Hotary KB, Allen ED, Brooks PC, Datta NS, Long MW, Weiss SJ. Membrane type I matrix metalloproteinase usurps tumor growth control imposed by the three-dimensional extracellular matrix. Cell 2003;114: 33–45.

20. Petty AP, Dick CL, Lindsey JS. Translation of an atypical human cDNA requires fidelity of a purine-pyrimidine repeat region and recoding. GENE 2008;414:49–59.

21. Wright SE, Kilinski L, Talib S, et al. Cytotoxic T lymphocytes from humans with adenocarcinomas stimulated by native MUC1 mucin and a mucin peptide mutated at a glycosylation site. J Immunother 2000;23: 2–10.

22. Hendrix MJC, Seftor EA, Seftor REB. Comparison of tumor cell invasion assays: human amnion versus reconstituted basement membrane barriers. Invasion Metastasis 1989;9:278–97.

23. Yang AD, Camp ER, Fan F, et al. Vascular endothelial growth factor receptor-1 activation mediates epithelial to mesenchymal transition in human pancreatic carcinoma cells. Cancer Res 2006;66:46–51.

24. Noguchi P. Use of flow cytometry for DNA analysis. In: Coligan J, Kruisbeek A, Margulies D, Shevach E, Strober W, editors. Current Protocols in Immunology. New York: Wiley-Interscience; 1991, p. 5.7.1–5.7.4.

25. Windsor LJ, Bodden MK, Birkedal-Hansen B, Engler JA, Birkedal-Hansen H. Mutational analysis of residues in and around the active site of human fibroblast-type collagenase. J Biol Chem 1994;269:26201–7.

26. Williams NS, Burgett AWG, Atkins AS, Wang X, Harran PG, McKnight SL. Therapeutic anticancer efficacy of a synthetic diazonamide analog in the absence of overt toxicity. Proc Natl Acad Sci U S A 2007;104: 2074–9.

27. Roehm NW, Rodgers GH, Hatfield SM, Glasebrook AL. An improved colorimetric assay for cell proliferation and viability utilizing the tetrazolium salt XTT. J Immunol Methods 1991;142:257–65.

28. Bae-Jump V, Segreti EM, Vandermolen D, Kauma S. Hepatocyte growth factor (HGF) induces invasion of endometrial carcinoma cell lines *in vitro*. Gynecol Oncol 1999;73:265–72.

29. Bescond A, Augier T, Chareyre C, Garcon D, Hornebeck W, Charpiot P. Influence of homocysteine on matrix metalloproteinase-2: activation and activity. Biochem Biophys Res Commun 1999;263:498–503.

30. Wart HEV, Birkedal-Hansen H. The cysteine switch: a principle of regulation of metalloproteinase activity with potential applicability to the entire matrix metalloproteinase gene family. Proc Natl Acad Sci U S A 1990; 87:5578–82.

31. Birkedal-Hansen H, Taylor RE. Detergent-activation of latent collagenase and resolution of its component molecules. Biochem Biophys Res Commun 1982;107:1173–8.

32. Wright SE, Rewers-Felkins KA, Quinlin IS, et al. Adoptive immunotherapy of mucin1 expressing adenocarcinomas with mucin1 stimulated human peripheral blood mononuclear cells. Int J Mol Med 2002;9: 401–4.

33. Rozanov DV, Deryugina EI, Ratnikov BI, et al. Mutation analysis of membrane type-1 matrix metalloproteinase (MT1-MMP). The role of the cytoplasmic tail Cys574, the active site Glu240, and furin cleavage motifs in oligomerization, processing, and self-proteolysis of MT1-MMP expressed in breast carcinoma cells. J Biol Chem 2001;276:25705–14.

34. Doerr ME, Jones JI. The roles of integrins and extracellular matrix proteins in the insulin-like growth factor I-stimulated chemotaxis of human breast cancer cells. J Biol Chem 1996;271:2443–7.

35. Silvestri I, Cattani IL, Franco P, et al. Engaged urokinase receptors enhance tumor breast cell migration and invasion by upregulating avb5 vitronectin receptor cell surface expression. Int J Cancer 2002;102: 562–71.

36. Nelson BH, Willerford DM. Biology of the interleukin-2 receptor. Adv Immunol 1998;70:1–81.

37. Celis JE, Moreira JMA, Gromova I, et al. Characterization of breast precancerous lesions and myoepithelial hyperplasia in sclerosing adenosis with apocrine metaplasia. Mol Oncol 2007;1:97–119.

38. Müller A, Homey B, Soto H, et al. Involvement of chemokine receptors in breast cancer metastasis. Nature 2001;410:50–6.

39. Lehti K, Lohi J, Valtanen H, Keski-Oja J. Proteolytic processing of membrane-type-1 matrix metalloproteinase is associated with gelatinase A activation at the cell surface. Biochem J 1998;334:345–53.

40. Sato H, Takino T, Okada Y, et al. A matrix metalloproteinase expressed on the surface of invasive tumour cells. Nature 1994;370:61–5.

41. Gingras D, Bousquet-Gagnon N, Langlois S, Lachambre M-P, Annabi B, Béliveau R. Activation of the extracellular signal-regulated protein kinase (ERK) cascade by membrane-type-1 matrix metalloproteinase (MT1-MMP). FEBS Lett 2001;507:231–6.

42. D'Alessio S, Ferrari G, Cinnante K, et al. Tissue inhibitor of metalloproteinases-2 binding to membrane-type 1 matrix metalloproteinase induces MAPK activation and cell growth by a non-proteolytic mechanism. J Biol Chem 2008;283:87–99.

43. Madhunapantula SV, Sharma A, Robertson GP. PRAS40 deregulates apoptosis in malignant melanoma. Cancer Res 2007;67:3626–36.

44. Hollier BG, Kricker JA, Van Lonkhuyzen DR, Leavesley DI, Upton Z. Substrate-bound insulin-like growth factor (IGF)-I-IGF binding protein-vitronectin-stimulated breast cell migration is enhanced by coactivation of the phosphatidylinositide 3-kinase/AKT pathway by {α}v-integrins and the IGF-I receptor. Endocrinology 2008;149:1075–90.

45. Matsuo M, Sakurai H, Ueno Y, Ohtani O, Saiki I. Activation of MEK/ERK and PI3K/Akt pathways by fibronectin requires integrin αv-mediated ADAM activity in hepatocellular carcinoma: a novel functional target for gefitinib. Cancer Sci 2006;97:155–62.

46. Zhou HY, Pon YL, Wong AST. Synergistic effects of epidermal growth factor and hepatocyte growth factor on human ovarian cancer cell invasion and migration: role of extracellular signal-regulated kinase 1/2 and p38 mitogen-activated protein kinase. Endocrinology 2007;148:5195–208.

47. Wong AST, Roskelley CD, Pelech S, Miller D, Leung PCK, Auersperg N. Progressive changes in Met-dependent signaling in a human ovarian surface epithelial model of malignant transformation. Exp Cell Res 2004; 299:248–56.

48. Lehti K, Allen E, Birkedal-Hansen H, et al. An MT1-MMP-PDGF receptor-{β} axis regulates mural cell investment of the microvasculature. Genes Dev 2005;19:979–91.

49. Takino T, Miyamori H, Watanabe Y, Yoshioka K, Seiki M, Sato H. Membrane type 1 matrix metalloproteinase regulates collagen-dependent mitogen-activated protein/extracellular signal-related kinase activation and cell migration. Cancer Res 2004;64:1044–9.

50. Tsubaki M, Matsuoka H, Yamamoto C, et al. The protein kinase C inhibitor, H7, inhibits tumor cell invasion and metastasis in mouse melanoma via suppression of ERK1/2. Clin Exp Metastasis 2007;24:431–8.

51. Bonta IL, Ben Efraim S. Interactions between inflammatory mediators in expression of antitumor cytostatic activity of macrophages. Immunol Lett 1990;25:295–301.

52. Xiang J, Moyana T, Qi Y. Genetic engineering of a recombinant fusion possessing anti-tumor F(ab')2 and tumor necrosis factor. J Biotechnol 1997;53:3–12.

53. Nyalendo C, Beaulieu E, Sartelet H, et al. Impaired tyrosine phosphorylation of membrane type 1-matrix metalloproteinase reduces tumor cell proliferation in three-dimensional matrices and abrogates tumor growth in mice. Carcinogenesis 2008;29:1655–64.

AACR American Association for Cancer Research

Molecular Cancer Therapeutics

Targeting Migration inducing gene-7 inhibits carcinoma cell invasion, early primary tumor growth, and stimulates monocyte oncolytic activity

Aaron P. Petty, Stephen E. Wright, Kathleen A. Rewers-Felkins, et al.

Updated version	Access the most recent version of this article at: doi:10.1158/1535-7163.MCT-09-0186

Cited articles	This article cites 52 articles, 16 of which you can access for free at: http://mct.aacrjournals.org/content/8/8/2412.full#ref-list-1
Citing articles	This article has been cited by 1 HighWire-hosted articles. Access the articles at: http://mct.aacrjournals.org/content/8/8/2412.full#related-urls

E-mail alerts	Sign up to receive free email-alerts related to this article or journal.
Reprints and Subscriptions	To order reprints of this article or to subscribe to the journal, contact the AACR Publications Department at pubs@aacr.org.
Permissions	To request permission to re-use all or part of this article, use this link http://mct.aacrjournals.org/content/8/8/2412. Click on "Request Permissions" which will take you to the Copyright Clearance Center's (CCC) Rightslink site.